Adaptive Temperature Monitoring for Battery Thermal Management

Ienkaran Arasaratnam*, Jimi Tjong†, Ryan Ahmed*, Mohammed El-Sayed* and Saeid Habibi*
*McMaster University
Hamilton, ON, Canada
Email: haran@ieee.org, ryan.ahmed@mcmaster.ca, abugabma@mcmaster.ca and habibi@mcmaster.ca
†University of Windsor
Windsor, ON, Canada
Email: jtjong@ford.com

***Abstract*—Battery thermal management is crucial for avoiding disastrous consequences due to short circuits and thermal runaway. The temperature inside a battery (core temperature) is higher than the temperature outside (skin temperature) under high discharge/charge rates. Although the skin temperature is measurable, the core temperature is not. In this paper, a lumped thermal model is considered to estimate the core temperature from skin temperature readings. To take into account uncertainties in thermal model parameters, which are bound to occur as the battery ages, an adaptive closed-loop estimation algorithm called the adaptive Potter filter is derived. Finally, computer simulations are performed to validate the adaptive Potter filter's ability to track the skin and core temperatures under high charge/discharge current pulses and model mismatches.**

***Index Terms*—Battery Thermal Management, Kalman Filter, Adaptive Estimation.**

I. Introduction

Like humans, batteries perform well at room temperature– any deviation towards high or low temperature adversely affects the availability of power, energy, charge acceptance during energy recovery from regenerative braking and battery life [7]. An improper temperature control may lead to thermal runaway. The main objective of a battery thermal management system is to ensure that the battery temperature and temperature deviation among cells and modules lie within an acceptable narrow operating range. To this end, the battery thermal management system uses various techniques such as cabin air cooling/heating, highly conductive active material and casing, optimized coolant baffle design, highly heat conductive coolant (typically liquid, phase change material or any combination), active cooling/heating and parallel cooling/heating [7], [10].

The existing methods used to predict/estimate the battery temperature distribution throughout the cell can be classified into two broad classes: High fidelity finite element models [4] and lumped thermal models [8]. For real-time onboard vehicle applications, we consider the latter class in this paper. Monitoring the core temperature is crucial because it is substantially higher than the skin temperature, specifically under high discharge rates. We propose a Bayesian algorithm called the adaptive Potter filter (APF) for the first time ever in the battery thermal management literature to estimate the core temperature from its skin temperature measurements. As the battery ages, battery model parameters (e.g., internal resistance) tend to drift; the adaptivity aspect of the APF is used to tackle model parameter uncertainties.

The rest of the paper is organized as follows: Section II lays a foundation for state-space modeling based on the lumped battery thermal model. Section III presents the APF algorithm. In Section IV, we demonstrate that the APF is capable of tracking the skin and core temperatures even when the thermal model parameters are not known accurately. Finally, Section V concludes the paper with some remarks.

II. State-Space Modeling based on a Lumped Thermal Model

The radially distributed thermal model of a cylindrical battery cell based on classical heat transfer theory can be approximately described by a pair of first-order partial differential equations [8], [9]:

$$\dot{T}_c = \frac{1}{C_c}\Big(\dot{s}_r + \frac{T_s - T_c}{R_c}\Big) \quad (1)$$

$$\dot{T}_s = \frac{1}{C_s}\Big(\frac{(T_f - T_s)}{R_u} - \frac{(T_s - T_c)}{R_c}\Big), \quad (2)$$

where T_s and T_c denote the skin temperature and the core temperature, respectively; T_f is the coolant temperature (see Fig. 1; The reader may refer to Table I for various cell-specific parameter definitions). The heat generation rate, $\dot{\mathbf{s}}_r$, in (1) can be calculated as follows:

$$\dot{s}_r = (OCV - V_T)I, \quad (3)$$

where the battery open-circuit voltage, OCV, is a function of the state-of-charge and temperature and V_T is the cell terminal voltage. The lumped model assumes that heat is generated from the core and zero flux at the center. Also, it neglects axial temperature variation and assumes a homogeneous condition.

A state-space model used for estimation consists of a couple of equations– (i) state equation and (ii) measurement equation. In our case, using (1)-(2), the state equation can be written in the following form:

$$\dot{\mathbf{x}} = \mathbf{A}\mathbf{x} + \mathbf{B}\mathbf{u}, \quad (4)$$

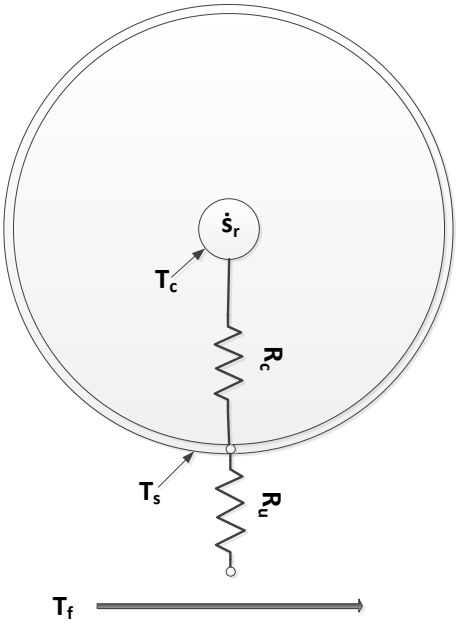

Fig. 1. Lumped Thermal Model of a Cylindrical Cell

where the state vector $\mathbf{x} = [T_c \ T_s]^T$; the state transition matrix

$$\mathbf{A} = \begin{pmatrix} \frac{-1}{R_c C_c} & \frac{1}{R_c C_c} \\ \frac{-1}{R_c C_s} & \frac{-1}{C_s}\left(\frac{1}{R_c} + \frac{1}{R_u}\right) \end{pmatrix}$$

the input matrix

$$\mathbf{B} = \begin{pmatrix} \frac{(OCV - V_t)}{C_c} & 0 \\ 0 & \frac{1}{R_u C_s} \end{pmatrix},$$

and the input $\mathbf{u} = [I \ \ T_f]^T$. Because the skin temperature, T_s, is measurable, we write the measurement equation as follows:

$$z = \mathbf{C}\mathbf{x}, \tag{5}$$

where $\mathbf{C} = [0 \ \ 1]$.

III. Adaptive Potter Filtering

To implement a continuous-time state-space model in a digital computer, it must first be converted to a discrete-time state-space model. If the charge/discharge current, voltage and temperature readings are available at distinct time instances, the discrete-time state-space model can be described by the following difference equations:

$$\mathbf{x}_{k+1} = \mathbf{A}_d \mathbf{x}_k + \mathbf{B}_d \mathbf{u}_k \tag{6}$$
$$z_k = \mathbf{C}\mathbf{x}_k, \tag{7}$$

where the time index $k = t/\Delta T$, t is the absolute time, and ΔT is the sampling time interval; the system and input matrices are given, respectively, as follows ([2]):

$$\mathbf{A}_d = \exp(\Delta T \mathbf{A})$$
$$\mathbf{B}_d = \mathbf{A}^{-1}(\mathbf{A}_d - \mathbf{I})\mathbf{B}.$$

In the Bayesian estimation framework, the posterior density of the state provides a complete statistical description of the state at that time. On the receipt of a new measurement at time instant k, the Bayesian filter updates the old posterior density of the state in two basic steps:

- *Time update*, which involves computing the predictive density
- *Measurement update*, which involves computing the posterior density of the current state

For a linear state-space model with additive Gaussian noise, the Kalman filter, which is one kind of the Bayesian filter, is the optimal estimator in a minimum mean squared-error sense. James H. Potter introduced a clever and efficient square-root counterpart of the Kalman filter when the measurement vector was single-dimensional. Potter's filter was successfully deployed in the lunar excursion module for the Apollo program half a century ago. Recently, it was applied by the authors to estimate the state-of-charge of Li-ion battery cells [2]. The motivation for a square-root formulation is that it always preserves the two basic properties of a covariance matrix, namely, symmetry and positive definiteness. In addition, the square-root algorithms are well known to provide increased stability especially when they are committed to hardware with limited precision [1]. Fortunately, in the context of the temperature estimation, because the skin temperature measurement is single dimensional, we adapt Potter's filter with little modifications.

A. Time Update

To take into account model mismatches and noisy current measurements, we rewrite the state equation (6) by adding noise as follows:

$$\boxed{\mathbf{x}_k = \mathbf{A}_d \mathbf{x}_{k-1} + \mathbf{B}_d \mathbf{u}_k + \mathbf{w}_k}, \tag{8}$$

where the process noise, $\mathbf{w}_k$, is assumed to be zero-mean Gaussian distributed, i.e., $\mathbf{w}_k \sim \mathcal{N}(\mathbf{0}, \mathbf{Q})$. At the end of this section, we will describe how to adaptively estimate $\mathbf{Q}$. Given that $\mathbf{x}_{k-1} \sim \mathcal{N}(\hat{\mathbf{x}}_{k-1|k-1}, \mathbf{P}_{k-1|k-1})$, we write the predicted state at time k as

$$\hat{\mathbf{x}}_{k|k-1} = \mathbb{E}[\mathbf{x}_k | z_1, z_2, \ldots z_{k-1}], \tag{9}$$

where $\mathbb{E}[.]$ is the expectation operator. Substituting (8) into (9) yields

$$\begin{aligned} \hat{\mathbf{x}}_{k|k-1} &= \mathbb{E}[\mathbf{A}_d \mathbf{x}_{k-1} + \mathbf{B}_d \mathbf{u}_{k-1} + \mathbf{w}_k | z_1, z_2, \ldots z_{k-1}] \\ &= \mathbf{A}_d \hat{\mathbf{x}}_{k-1|k-1} + \mathbf{B}_d \mathbf{u}_{k-1}. \end{aligned} \tag{10}$$

Due to the fact that deriving the square-root of the predicted state-error covariance is mathematically involved, we first introduce the following notations:

- We shall use $\mathbf{S}_Q$ for square root of the process noise covariance $\mathbf{Q}$.
- A covariance matrix $\mathbf{P}$ can be written in a squared-form, as shown by [1]:

$$\mathbf{P} = \mathbf{S}_o \mathbf{S}_o^T, \tag{11}$$

where $\mathbf{P} \in \mathbb{R}^{n\times n}$, $\mathbf{S_o} \in \mathbb{R}^{n\times m}$, $m > n$, is a 'fat' matrix. Though $\mathbf{S}_o$ in (11) can be considered as a square-root of $\mathbf{P}$, we prefer to keep the square-root as an $n\times n$ triangular matrix for computational reasons. The transformation of $\mathbf{S}_o$ into a triangular matrix $\mathbf{S}_n \in \mathbb{R}^{n\times n}$ is performed by a triangularization procedure (e.g., Gram-Schmidt based QR-decomposition). When the matrix $\mathbf{S}_o^T$ is decomposed into an orthogonal matrix $\mathbf{V} \in \mathbb{R}^{m\times n}$ and an upper triangular matrix $\mathbf{D} \in \mathbb{R}^{n\times n}$ such that $\mathbf{S}_o^T = \mathbf{VD}$, we get

$$\mathbf{P} \quad = \quad \mathbf{S}_o\mathbf{S}_o^T = \mathbf{D}^T\mathbf{V}^T\mathbf{VD} = \mathbf{D}^T\mathbf{D} = \mathbf{S}_n\mathbf{S}_n^T,$$

where the 'new' square-root of $\mathbf{P}$, $\mathbf{S}_n = \mathbf{D}^T$. In this paper, we simplify matters by using the notation

$$\mathbf{S}_n \quad = \quad \textbf{Tria}(\mathbf{S}_o),$$

where $\mathbf{S}_o$ is referred to as the 'old' square-root of $\mathbf{P}$.

Now, we write the predicted error covariance

$$\begin{aligned}\mathbf{P}_{k|k-1} &= \text{Cov}[\mathbf{x}_k|z_1, z_2, \ldots z_{k-1}] \\ &= \text{Cov}[\mathbf{A}_d\mathbf{x}_{k-1} + \mathbf{B}_d\mathbf{u}_{k-1} + \mathbf{w}_k|z_1, z_2, \ldots z_{k-1}] \\ &= \mathbf{A}_d\mathbf{P}_{k|k-1}\mathbf{A}_d^T + \mathbf{Q}, \end{aligned} \tag{12}$$

Using the square-root factor of $\mathbf{Q}$ and rearranging matrices cleverly, we rewrite (12) as

$$\begin{aligned}\mathbf{P}_{k|k-1} &= (\mathbf{A}_d\mathbf{S}_{k|k-1})(\mathbf{A}_d\mathbf{S}_{k|k-1})^T + \mathbf{S_Q}\mathbf{S}_Q^T \\ &= [\mathbf{A}_d\mathbf{S}_{k|k-1} \quad \mathbf{S}_Q][\mathbf{A}_d\mathbf{S}_{k|k-1} \quad \mathbf{S}_Q]^T.\end{aligned}$$

Hence, using the triangularization theory mentioned above, the square-root factor of the predicted state-error covariance can be written as

$$\mathbf{S}_{k|k-1} \quad = \quad \textbf{Tria}([\mathbf{A}_d\mathbf{S}_{k|k-1} \quad \mathbf{S}_Q]).$$

B. Measurement Update

To take into account model mismatches and stochastic factors, similarly to the state equation, we rewrite the measurement equation (7) by adding noise as follows:

$$\boxed{z_k = \mathbf{C}\mathbf{x}_k + e_k}, \tag{13}$$

where the measurement noise, e_k, is assumed to be zero-mean Gaussian distributed, i.e., $e_k \sim \mathcal{N}(0, \sigma_e^2)$. Typically, the standard deviation of voltage measurement errors, σ_e, can be deduced from the precision of a thermocouple. Since the measurement is single dimensional, we adopt Potter's idea to derive the measurement update (see APPENDIX).

C. Q-Adaptive Time Update

To take into account model mismatches and stochastic noise sources, we adaptively estimate the process noise covariance, $\mathbf{Q}$, by closely following the idea presented by Maybeck in [6]. The basic premise is to use the measurement residuals to modify $\mathbf{Q}$. Maybeck derives the process noise covariance update equation by setting up a moving window of length N as follows:

$$\begin{aligned}\hat{\mathbf{Q}} &= \frac{1}{N}\sum_{i=k-N+1}^{k}\Big[\Delta\mathbf{x}_i\Delta\mathbf{x}_i^T - \\ &\qquad \big(\mathbf{A}_d\mathbf{P}_{i-1|i-1}\mathbf{A}_d^T - \mathbf{P}_{i|i} + \hat{\mathbf{Q}}_{i-1}\big)\Big]\end{aligned} \tag{14}$$

where the measured state residual at the time instant i is given by

$$\Delta\mathbf{x}_i \quad = \quad \hat{\mathbf{x}}_{i|i} - \hat{\mathbf{x}}_{i|i-1}$$

The term $\Delta\mathbf{x}_i$ represents the difference between the state estimate before the measurement update and after the measurement update and $\mathbf{P}_{i|i}$ refers to the updated state error covariance at time index i. Equation (14) lies at the heart of the Q-adaptive algorithm. If the residual is large, then the filter prediction is considered to be inaccurate. However, as the filter converges, the residual decreases and the filter's ability to predict the next state improves.

Using the fact that

$$\mathbf{P}_{i|i-1} \quad = \quad \mathbf{A}_d\mathbf{P}_{i-1|i-1}\mathbf{A}_d^T + \hat{\mathbf{Q}}_{i-1}$$

(14) can be rewritten as

$$\hat{\mathbf{Q}} \quad = \quad \frac{1}{N}\sum_{i=k-N+1}^{k}\Big[\Delta\mathbf{x}_i\Delta\mathbf{x}_i^T - \big(\mathbf{P}_{i|i-1} - \mathbf{P}_{i|i}\big)\Big] \tag{15}$$

Equation (15) shows explicitly that $\hat{\mathbf{Q}}$ equals the measured state residual minus the change in the a posteriori covariances due to the measurement update. A practical limitation of using (15) to estimate the process noise is that it is not guaranteed to be positive definite. Consequently, we rewrite (15) approximately as

$$\hat{\mathbf{Q}} \quad \approx \quad \frac{1}{N}\sum_{i=k-N+1}^{k}\Delta\mathbf{x}_i\Delta\mathbf{x}_i^T \tag{16}$$

In the course computing the estimates of the process noise covariance matrices, it is useful to combine the current estimate with the past to smooth the estimate histories as follows:

$$\hat{\mathbf{Q}}_k \quad = \quad \lambda\hat{\mathbf{Q}}_{k-1} + (1-\lambda)\hat{\mathbf{Q}} \tag{17}$$

Typically, we set λ to be $1 > \lambda > 0.95$. If λ is small, then each update has a large impact. On the other hand, if λ is large, then each update has only a small effect on the updated state. In a nutshell, the Potter filter includes $\mathbf{Q}$ in its time update that is adaptively calculated using Maybeck's idea.

IV. Computer Experiments

We performed a computer simulation to evaluate the adaptive Potter filter (APF) and compared it with open loop prediction (OLP). To simulate a battery, we used a simple OCV-R-RC-RC equivalent circuit electrical model coupled with the thermal model through heat generation as described in Section II. The thermal model used the parameter values listed under the 'True' column of Table I. During estimation, only the thermal model with the parameters shown under the

'Estimate' column of Table I was assumed; heat generation was approximately calculated by the formula $I^2\hat{R}_e$. The battery was excited with a current pulse as shown in Fig. 2– The current profile consists of a series of charging and discharging events for 40 minutes followed by rest for another 40 minutes. The data were collected at every 0.5 seconds. The air (coolant) temperature T_f was assumed to be $25°C$.

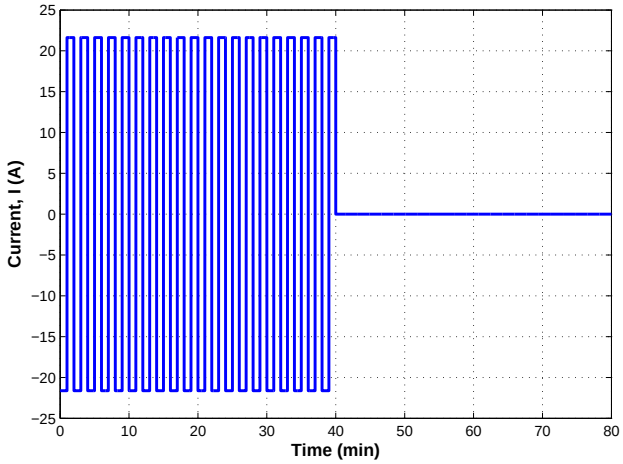

Fig. 2. Current Profile Used to Excite the Cell

As can be seen from Figs. 3(a)-3(b), the core temperature (T_c) seems to be $7°C$ higher than the skin temperature (T_s), approximately and falls down during the rest period and approaches T_s. T_c reaches $37°C$ at the end of charge/discharge cycle, whereas T_s increases up to $29.5°C$ at maximum. Figs. 3(a)-3(b) also show that the OLP fails to track both T_s and T_c accurately. The failure is attributed to the model mismatches. However, the APF tracks T_s and T_c closely, although T_c estimated by the APF deviates less than $1°C$ from the true. The APF's successful survival can be attributed to its adaptivity and feedback loop. In a nutshell, the observations drawn from this simulation study substantiate our belief that the APF is capable of tracking T_s and T_c even when the thermal model parameters are not known accurately (The reader may refer to https://sites.google.com/site/haranarasaratnam/software for a set of Matlab code used to generate the results).

V. Concluding Remarks

It is crucial to estimate the core temperature of a battery cell accurately because it must be kept below a maximum allowable limit. To this end, for the first time ever in the literature, this paper has combined Potter's filter with Maybeck's adaptive estimation strategy to derive a Q-adaptive Potter filtering algorithm for estimating the skin and core temperatures of a battery cell. It was successfully demonstrated that the Q-adaptive Potter filter is capable of closely tracking the true core and skin temperatures (with an error of less than a degree Celsius). This observation also suggests that the adaptive Potter filter is likely to survive even when the battery ages and its parameters drift from the assumed values. The following two research topics are currently under our investigation: (i) Extending the Potter filter for thermal management in a cluster of battery cells, (ii) Design of a battery thermal management system using coupled electrochemical-thermal models. Our objective is to finally apply these techniques to real (H)EV battery packs.

Appendix
Potter Filtering Algorithm

For completeness, we present the time and measurement update steps of the Potter filter below. For a detailed derivation of Potter's filter, the reader may consult [3].

Time Update

1) Assume at time k that the posterior density function $p(\mathbf{x}_{k-1}|z_1, z_2, \ldots z_{k-1}) = \mathcal{N}(\hat{\mathbf{x}}_{k-1|k-1}, \mathbf{P}_{k-1|k-1})$ is known. Estimate the predicted state

$$\hat{\mathbf{x}}_{k|k-1} = \mathbf{A}_d\hat{\mathbf{x}}_{k-1|k-1} + \mathbf{B}_d\mathbf{u}_{k-1} \quad (18)$$

2) Estimate the square-root factor of the predicted state-error covariance

$$\mathbf{S}_{k|k-1} = \mathbf{Tria}\Big([\mathbf{A}_d\mathbf{S}_{k-1|k-1} \quad \mathbf{S}_Q]\Big) \quad (19)$$

Measurement Update

1) Calculate the vector

$$\mathbf{T}_k = \mathbf{S}_{k|k-1}^T\mathbf{C}^T, \quad (20)$$

2) Calculate the scalar

$$\alpha_k = \frac{1}{\mathbf{T}_k^T\mathbf{T}_k + \sigma_e^2} \quad (21)$$

3) Estimate the filter gain

$$\mathbf{W}_k = \alpha_k\mathbf{S}_{k|k-1}\mathbf{T}_k \quad (22)$$

4) Estimate the predicted measurement

$$\hat{z}_{k|k-1} = \mathbf{C}\hat{\mathbf{x}}_{k|k-1} \quad (23)$$

5) Estimate the updated state

$$\hat{\mathbf{x}}_{k|k} = \hat{\mathbf{x}}_{k|k-1} + \mathbf{W}_k(z_k - \hat{z}_{k|k-1}) \quad (24)$$

6) Calculate the scalar

$$\gamma_k = \frac{1}{1 + \sigma_e\sqrt{\alpha_k}} \quad (25)$$

7) Estimate the square-root factor of the updated state-error covariance

$$\mathbf{S}_{k|k} = \mathbf{S}_{k|k-1} - \gamma_k\mathbf{W}_k\mathbf{T}_k^T \quad (26)$$

References

[1] I. Arasaratnam, S. Haykin, and T. Hurd, "Cubature Kalman Filtering for Continuous-Discrete Systems: Theory and Simulations," *IEEE Trans. Signal Processing*, 58(10), pp. 4977-4993, Oct. 2010.

[2] I. Arasaratnam, R. Ahmed, M. El-Sayed, J. Tjong, and S. Habibi, "Li-ion Battery SoC Estimation Using a Bayesian Tracker," *SAE* Technical Paper, 2013-01-153, April 2013.

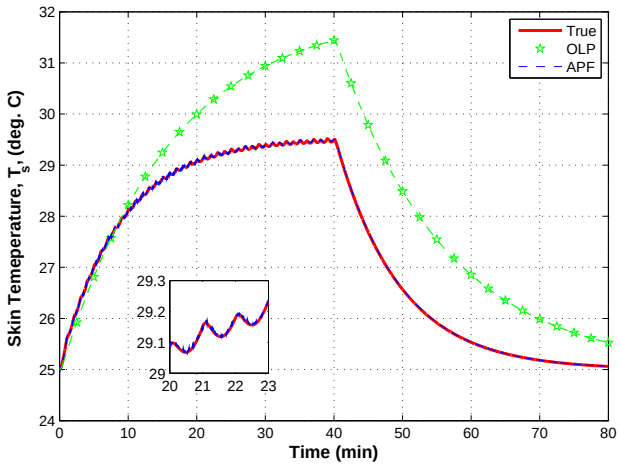

(a) Skin Temperature Profile

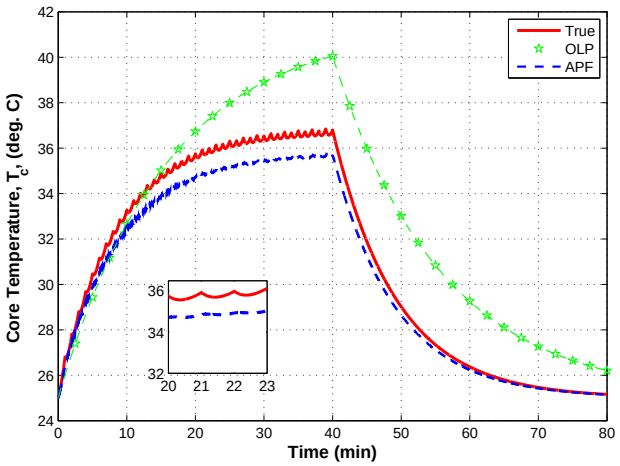

(b) Core Temperature Profile

Fig. 3. Actual temperature profiles and their estimation using two different methods– (i) Open loop prediction (OLP) (ii) Adaptive Potter filter (APF)

[3] G. H. Born, "Potter Square Root Filter", ASEN 5070 Course Handout, University of Colorado at Boulder, http://ccar.colorado.edu/ASEN5070/handouts.htm, viewed Sept. 16, 2012.

[4] G-H. Kim, & A. Pesaran,"Battery thermal management system design modeling," National Renewable Energy Laboratory, 2006.

[5] U-S Kim, C-B. Shin, & C-S. Kim, "Effect of electrode configuration on the thermal behavior of a lithium-polymer battery" *Journal of Power Sources* , 180(2), 909-916, 2008.

[6] P. S. Maybeck, *Stochastic models, estimation and control*, Mathemeatics and Science Engineering, 1979.

[7] A. Pesaran, "Battery Thermal Management In EVs And HEVs: Issues and Solutions" *Battery Man.*, 43(5), 2001.

[8] C. Park & A. K. Jaura, "Dynamic thermal model of li-ion battery for predictive behavior in hybrid and fuel cell vehicles,", *SAE transactions*, 112(3), 1835-1842, 2003.

[9] X. Lin, H. E. Perez, J. B. Siegel, A. Stefanopoulou, Y. Ding, & M. P. Castanier, "Parameterization and observability analysis of scalable battery clusters for onboard thermal management," Army Tank Automotive Research Develeopment and Engineering Center, Warren, MI, 2011.

[10] Z. Rao, & S. Wang, "A review of power battery thermal energy management", *Renewable and Sustainable Energy Reviews*, 2011.

TABLE I
CELL PARAMETERS

Name	**Symbol**	**Unit**	**True**	**Estimate**
Conduction resistance	R_c	$^\circ C/W$	1.26	2
Heat capacity at core	C_c	J/K	268	270
Convection resistance	R_u	$^\circ C/W$	0.8	1.5
Heat capacity at skin	C_s	J/K	18.8	19
Electric resistance	R_e	$m\Omega$	-	10